

Wen Yang, Kan Li, Yuwei Bai,
Ruimin Zhou, Weihong Zhou*
and Mark Bartlam*

Tianjin Key Laboratory of Protein Science,
College of Life Sciences, Nankai University,
Tianjin 300071, People's Republic of China

Correspondence e-mail:
zhouwh@nankai.edu.cn,
bartlam@nankai.edu.cn

Received 30 March 2010
Accepted 25 August 2010

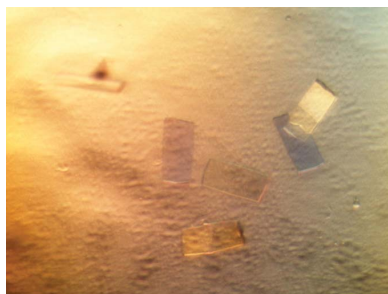
Expression, purification, crystallization and preliminary crystallographic analysis of PA3885 (TpbA) from *Pseudomonas aeruginosa* PAO1

Biofilms are important in cell communication and growth in most bacteria and are also responsible for most human clinical infections and diseases. Quorum-sensing systems have been identified to be crucial for biofilm formation and regulation. PA3885 (TpbA), a tyrosine phosphatase, is reported to convert extracellular quorum-sensing signals into internal gene-cascade reactions that result in reduced biofilm formation in the opportunistic pathogen *Pseudomonas aeruginosa*. Here, PA3885 from *P. aeruginosa* PAO1 was expressed, purified and crystallized. Single crystals were studied by X-ray crystallography and native diffraction data were collected to 2.8 Å resolution. These crystals were determined to belong to space group C2. It was not possible to conclusively determine the number of proteins in the asymmetric unit from the preliminary X-ray diffraction data analysis alone and attempts to determine the crystal structure of PA3885 are currently under way.

1. Introduction

As an opportunistic pathogen with metabolic versatility, *Pseudomonas aeruginosa* can be found in a wide variety of environments, including water, soil and various organisms, and can cause disease in plants, animals and humans (Oberhardt *et al.*, 2008). Immuno-compromised patients and those with cystic fibrosis are at particularly high risk of infection by *P. aeruginosa*, which can cause acute life-threatening infections (Prince, 2002). The mucoid phenotype can provide *P. aeruginosa* with an advantage in resisting phagocytosis (Mahenthiralingam *et al.*, 1994). Moreover, *P. aeruginosa* has a high drug resistance as a consequence of the membrane-permeability barrier (Sakharkar *et al.*, 2009), which renders it difficult to treat patients infected with this pathogen. *P. aeruginosa* has attracted considerable attention in both the basic research and clinical arenas owing to its considerable morbidity and mortality, and efforts have been made to explore more efficient treatments for *P. aeruginosa* infection.

Biofilm formation in *P. aeruginosa* is the crucial step in the establishment of chronic infections and persistence in the host and is also responsible for cell communication and growth (Costerton *et al.*, 1999; O'Toole & Kolter, 1998). Quorum sensing, as a mechanism of communication to coordinate behaviour, has been found to have an influence on biofilm formation (Winstanley & Fothergill, 2009; Dickschat, 2010) and requires a large network of genes for regulation (Passador *et al.*, 1993; Ochsner & Reiser, 1995; Diggle *et al.*, 2006). Recently, PA3885 (TpbA) from *P. aeruginosa* PA14 has been reported to be secreted to the periplasm and to link the extracellular quorum-sensing signals to EPS (extracellular polysaccharide) production and biofilm formation *via* negative regulation of c-di-GMP (3',5'-cyclic diguanylic acid; Ueda & Wood, 2009), which is well known to regulate biological processes, including motility and biofilm formation in bacteria (Nakhmachik *et al.*, 2008). Loss or mutation of PA3885 can decrease swimming, abolish swarming and increase aggregation. PA3885 has a conserved tyrosine phosphatase domain, and relevant phosphatase activities with *p*-nitrophenylphosphate



© 2010 International Union of Crystallography
All rights reserved

(pNPP) and phosphotyrosine peptides have been reported (Ueda & Wood, 2009). PA3885 has the ability to dephosphorylate a GGDEF protein, PA1120 (TpbB), at two periplasmic tyrosine residues and in turn cause c-di-GMP production to be reduced. This will further influence a number of properties of *P. aeruginosa* and eventually suppress biofilm production, as well as enhance swarming motility (Ueda & Wood, 2009). Therefore, PA3885 may function as a balancing factor between biofilm formation and motility in *P. aeruginosa*.

As an important connection between extracellular quorum-sensing signals and biofilm formation, PA3885 may be a potential target for controlling bacterial social behaviour and even drug development (Wang & Xu, 2010). Furthermore, PA3885 functions as a member of the PTP (protein tyrosine phosphatase) superfamily, which may have a range of substrates and even several inhibitors (Alonso *et al.*, 2004; Aceti *et al.*, 2008). There are no homologous structures with high similarity to PA3885 in the Protein Data Bank, but two proteins that share relatively low sequence identity are At1g05000 from *Arabidopsis thaliana* (PDB code 1xri; 22% sequence identity; Aceti *et al.*, 2008) and VHR from *Homo sapiens* (PDB code 1vhr; 24% sequence identity; Yuvaniyama *et al.*, 1996). The three-dimensional structure of PA3885 should therefore help to elucidate the active-site architecture and substrate specificity, thus providing a basis for inhibitor design. Here, we report the expression, purification and crystallization of PA3885 from *P. aeruginosa* PAO1. Diffraction data from a PA3885 crystal were collected to 2.8 Å resolution. The crystal belonged to space group *C2*, with unit-cell parameters $a = 39.0$, $b = 233.6$, $c = 84.5$ Å, $\alpha = \gamma = 90$, $\beta = 96.2^\circ$.

2. Materials and methods

2.1. Cloning, expression and purification

The gene encoding PA3885 (Gene ID 878776; residues 29–218) from *P. aeruginosa* PAO1 was amplified from the genome of *P. aeruginosa* PAO1 and then inserted into the expression vector pGEX-6P-1 (GE Healthcare) using the *Bam*HI and *Xho*I restriction sites and with an N-terminal glutathione *S*-transferase (GST) tag. The recombinant plasmid was transformed into *Escherichia coli* strain BL21 (DE3) and a single colony was cultured in LB medium at 310 K with 50 µg ml⁻¹ ampicillin to an OD₆₀₀ of 0.6–0.8 and then induced with 0.5 mM isopropyl β-D-1-thiogalactopyranoside (IPTG) for 18 h

at 289 K. The cells were harvested by centrifugation, resuspended in 1 × PBS buffer and lysed by sonication at 277 K. The supernatant obtained by centrifugation at 27 000g for 30 min was loaded onto a glutathione-affinity column (GE Healthcare) pre-equilibrated with 1 × PBS buffer. Contaminant protein was washed off with 200 ml 1 × PBS buffer and the glutathione *S*-transferase (GST) fusion protein was cleaved with PreScission Protease (GE Healthcare) overnight at 277 K. The desired protein was eluted from the column with about 10 ml 1 × PBS buffer. The protein was concentrated by ultrafiltration and applied onto a Superdex-75 (GE Healthcare) chromatography column in 1 × PBS buffer. The peak was collected and concentrated to 500 µl in buffer *A* (20 mM Tris pH 8.0). Further purification was achieved by Resource Q anion-exchange chromatography (GE Healthcare) and the target protein was finally eluted using a linear gradient of 0–0.5 M NaCl in buffer *A*. The purity of the PA3885 was estimated to be greater than 95% by SDS–PAGE analysis.

2.2. Crystallization

The purified PA3885 protein was concentrated to 30 mg ml⁻¹ in a buffer consisting of 20 mM Tris pH 8.0, 150 mM NaCl, 10 mM β-mercaptoethanol. Crystallization was performed by the sitting-drop vapour-diffusion method at 293 K; 1 µl protein solution (30 mg ml⁻¹) was mixed with 1 µl well solution and equilibrated over 100 µl well solution. Crystal screening was carried out with Hampton Research Crystal Screen, Crystal Screen 2 and Index kits in 48-well plates (XtalQuest). Initial twinned crystals of PA3885 were obtained from Crystal Screen condition No. 48 (2 M ammonium phosphate monobasic, 0.1 M Tris pH 8.5) and further optimization was performed by varying the buffer pH and the concentration of precipitant and by additive screening. Fortunately, after two weeks good-quality crystals were grown under the optimized conditions of 1.7 M ammonium phosphate monobasic, 0.1 M Tris pH 8.1 with 7% (v/v) polyethylene glycol (PEG) 400 as an additive (Fig. 1).

2.3. Data collection and processing

Immediately prior to data collection, the PA8335 crystals were cryoprotected for about 10 s by the addition of 20% (v/v) glycerol to the crystallization conditions. X-ray diffraction data were collected in-house on a Rigaku R-Axis HTC image plate using Cu *K*α radiation ($\lambda = 1.5418$ Å) from an in-house Rigaku MicroMax-007 HF

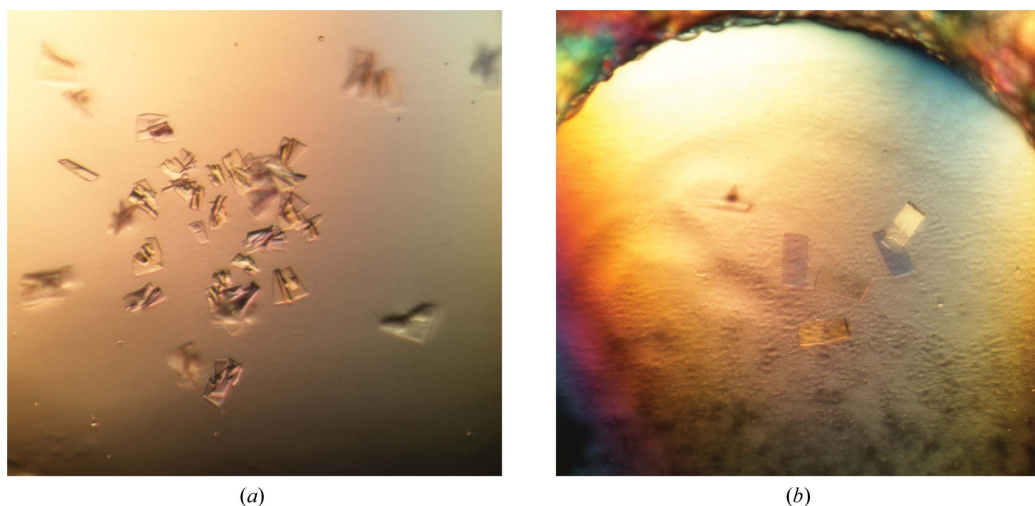


Figure 1 Crystals of PA3885. (a) Twinned crystals without additive screening. (b) Single crystals with a low concentration of PEG 400 as an additive (estimated dimensions of 150 × 50 × 20 µm).

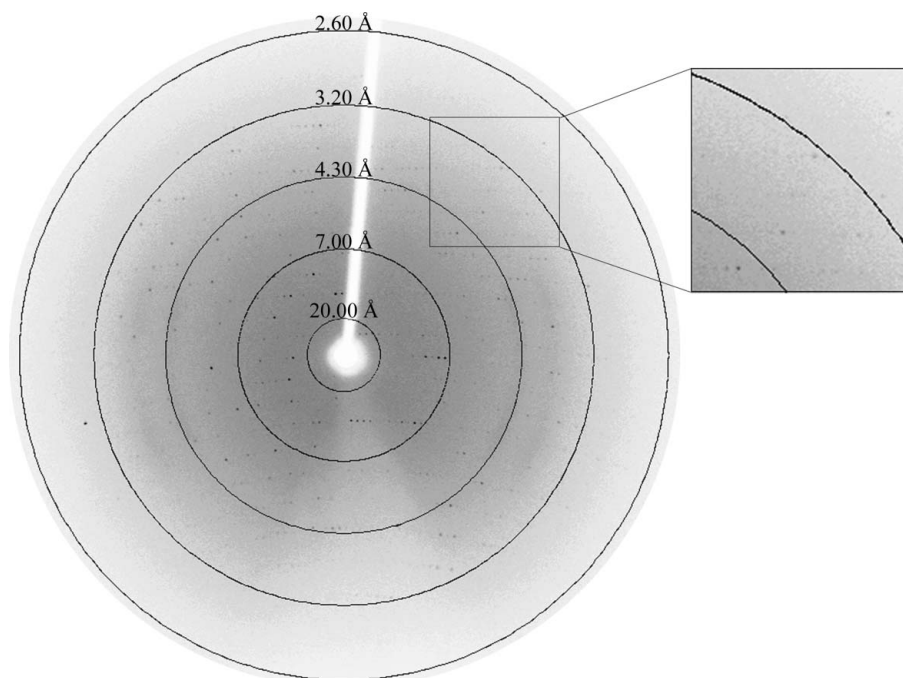


Figure 2

A typical diffraction pattern from a PA3885 crystal collected on a Rigaku R-AXIS HTC image plate.

rotating-anode X-ray generator operating at 40 kV and 30 mA (Fig. 2). All diffraction data were indexed, integrated and merged using the *HKL-2000* suite (Otwinowski & Minor, 1997). Complete data-collection statistics are summarized in Table 1.

3. Results and discussion

The PA3885 gene from *P. aeruginosa* PAO1 encodes a protein of 218 amino acids that has been reported to be a tyrosine phosphatase targeting PA1120 (TpbB) in the periplasm (Ueda & Wood, 2009). Therefore, the PA3885 protein has an N-terminal 28-amino-acid signal peptide that is necessary for secretion. We subsequently cloned the PA3885 gene from residues 29–218 into the pGEX-6P-1 vector, minus the signal peptide, to facilitate its expression and crystallization. After cleavage with PreScission protease the target protein has an additional five residues (-GPLGS-) at the N-terminus and was used for further purification and crystallization.

Crystal Screen, Crystal Screen 2 and Index kits (Hampton Research) were used for preliminary screening and several crystals were obtained from Crystal Screen condition No. 48. The crystals remained twinned after adjustment of the buffer, the pH and the concentration of precipitant. However, fine single well diffracting crystals were obtained by adding a low concentration [5–10% (v/v)] of PEG 400 as an additive (Fig. 1). The diffraction data reached a maximum of 2.8 Å resolution using a home X-ray source.

The PA3885 crystal belonged to space group *C2*, with unit-cell parameters $a = 39.0$, $b = 233.6$, $c = 84.5$ Å, $\alpha = \gamma = 90$, $\beta = 96.2^\circ$. Attempts to determine the exact number of protein molecules in one asymmetric unit were inconclusive. We speculate that three or four protein molecules may be reasonable, with respective Matthews coefficients of 3.04 and 2.28 Å³ Da⁻¹ (Matthews, 1968) calculated using the *CCP4* suite (Collaborative Computational Project, Number 4, 1994). The self-rotation function ($\kappa = 180^\circ$) shows orthogonal peaks at 90° , suggesting the presence of four molecules in the asymmetric unit (Fig. 3).

We attempted to use At1g05000 (PDB code 1xri; 22% sequence identity for 128 residues) and VHR (PDB code 1vhr; 24% sequence identity for 132 residues) as initial search models to determine the phases of PA3885 by molecular replacement. We also tried all seven possible solvent contents using *CNS* v.1.2 (Brünger *et al.*, 1998) and *Phaser* (McCoy *et al.*, 2007). Unfortunately, no correct molecular-replacement solution was found owing to the low similarity in primary sequence and a possible large diversity in structure. Therefore, we are currently preparing a selenomethionyl derivative of

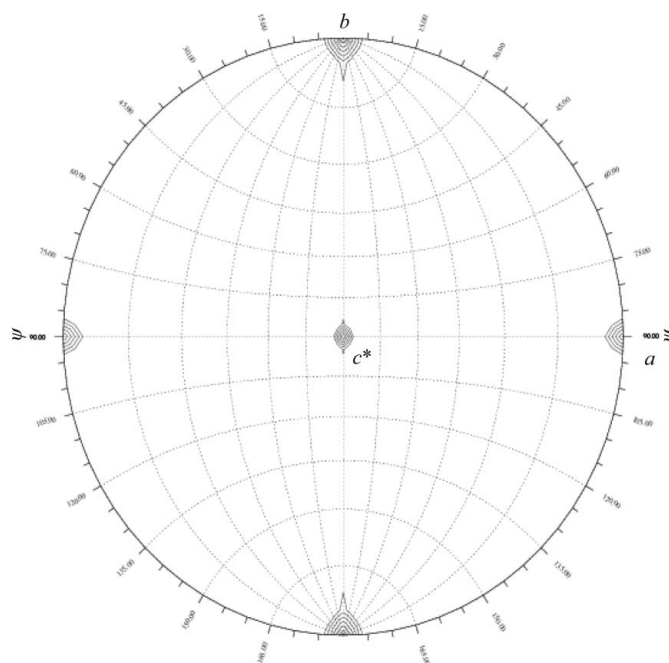


Figure 3

The self-rotation function ($\kappa = 180^\circ$).

Table 1

Data-collection and processing statistics for PA3885.

Values in parentheses are for the highest resolution shell.

No. of crystals	1
Generator	Rigaku MicroMax-007 HF
Wavelength (Å)	1.5418
Detector	Rigaku R-Axis HTC
Crystal-to-detector distance (mm)	200
Rotation range per image (°)	0.5
Total rotation range (°)	180
Exposure time per image (s)	300
Resolution range (Å)	50.0–2.8 (2.85–2.80)
Space group	C2
Unit-cell parameters (Å, °)	$a = 39.0, b = 233.6, c = 84.5,$ $\alpha = 90.0, \beta = 96.2, \gamma = 90.0$
Mosaicity (°)	1.53
Total No. of measured intensities	64196
Unique reflections	17939
Multiplicity	3.6 (3.4)
Mean $I/\sigma(I)$	13.0 (3.0)
Completeness (%)	96.7 (94.7)
$R_{\text{merge}}^{\dagger}$ (%)	13.4 (52.7)
Overall B factor from Wilson plot (Å ²)	46.3

$\dagger R_{\text{merge}} = \frac{\sum_{hkl} \sum_i |I_i(hkl) - \langle I(hkl) \rangle|}{\sum_{hkl} \sum_i I_i(hkl)}$, where $\langle I(hkl) \rangle$ is the mean intensity of the observations $I_i(hkl)$ of reflection hkl .

PA3885 with a view to solving the phase problem by multiple-wavelength anomalous dispersion. The PA3885 structure should provide valuable information on the crystallographic parameters, active-site architecture and substrate specificity.

We thank Professor Mingqiang Qiao for kindly supplying the genome of *P. aeruginosa* PAO1. This work was supported by grant 2007CB914301 from the Ministry of Science and Technology of China Project 973 (to MB and WZ).

References

- Aceti, D. J., Bitto, E., Yakunin, A. F., Proudfoot, M., Bingman, C. A., Frederick, R. O., Sreenath, H. K., Vojtik, F. C., Wrobel, R. L., Fox, B. G., Markley, J. L. & Phillips, G. N. Jr (2008). *Proteins*, **73**, 241–253.
- Alonso, A., Sasin, J., Bottini, N., Friedberg, I., Osterman, A., Godzik, A., Hunter, T., Dixon, J. & Mustelin, T. (2004). *Cell*, **117**, 699–711.
- Brünger, A. T., Adams, P. D., Clore, G. M., DeLano, W. L., Gros, P., Grosse-Kunstleve, R. W., Jiang, J.-S., Kuszewski, J., Nilges, M., Pannu, N. S., Read, R. J., Rice, L. M., Simonson, T. & Warren, G. L. (1998). *Acta Cryst.* **D54**, 905–921.
- Collaborative Computational Project, Number 4 (1994). *Acta Cryst.* **D50**, 760–763.
- Costerton, J. W., Stewart, P. S. & Greenberg, E. P. (1999). *Science*, **284**, 1318–1322.
- Dickschat, J. S. (2010). *Nat. Prod. Rep.* **27**, 343–369.
- Diggle, S. P., Cornelis, P., Williams, P. & Camara, M. (2006). *Int. J. Med. Microbiol.* **296**, 83–91.
- Mahenthalingam, E., Campbell, M. E. & Speert, D. P. (1994). *Infect. Immun.* **62**, 596–605.
- Matthews, B. W. (1968). *J. Mol. Biol.* **33**, 491–497.
- McCoy, A. J., Grosse-Kunstleve, R. W., Adams, P. D., Winn, M. D., Storoni, L. C. & Read, R. J. (2007). *J. Appl. Cryst.* **40**, 658–674.
- Nakhmchik, A., Wilde, C. & Rowe-Magnus, D. A. (2008). *Appl. Environ. Microbiol.* **74**, 4199–4209.
- Oberhardt, M. A., Puchalka, J., Fryer, K. E., Martins dos Santos, V. A. & Papin, J. A. (2008). *J. Bacteriol.* **190**, 2790–2803.
- Ochsner, U. A. & Reiser, J. (1995). *Proc. Natl Acad. Sci. USA*, **92**, 6424–6428.
- O'Toole, G. A. & Kolter, R. (1998). *Mol. Microbiol.* **30**, 295–304.
- Otwinowski, Z. & Minor, W. (1997). *Methods Enzymol.* **276**, 307–326.
- Passador, L., Cook, J. M., Gambello, M. J., Rust, L. & Iglewski, B. H. (1993). *Science*, **260**, 1127–1130.
- Prince, A. S. (2002). *N. Engl. J. Med.* **347**, 1110–1111.
- Sakharkar, M. K., Jayaraman, P., Soe, W. M., Chow, V. T., Sing, L. C. & Sakharkar, K. R. (2009). *J. Microbiol. Immunol. Infect.* **42**, 364–370.
- Ueda, A. & Wood, T. K. (2009). *PLoS Pathog.* **5**, e1000483.
- Wang, W. M. & Xu, Z. H. (2010). *Zhejiang Da Xue Xue Bao Yi Xue Ban*, **39**, 103–108.
- Winstanley, C. & Fothergill, J. L. (2009). *FEMS Microbiol. Lett.* **290**, 1–9.
- Yuvaniyama, J., Denu, J. M., Dixon, J. E. & Saper, M. A. (1996). *Science*, **272**, 1328–1331.